Estimating total horizontal aeolian flux within shrub-invaded groundwater-dependent meadows using empirical and mechanistic models

Kimberly R. Vest,[1] Andrew J. Elmore,[1] James M. Kaste,[2] Gregory S. Okin,[3] and Junran Li[3]

Received 7 December 2011; revised 12 February 2013; accepted 15 February 2013; published 21 June 2013.

[1] Wind erosion is a significant environmental problem that removes soil resources from sensitive ecosystems and contributes to air pollution. In regions of shallow groundwater, friable (puffy) soils are maintained through capillary action, surface evaporation of solute-rich soil moisture, and protection from mobilization by groundwater-dependent grasses and shrubs. When a reduction in vegetation cover occurs through any disturbance process, there is potential for aeolian transport and dust emission. We find that as mean gap size between vegetation elements scaled by vegetation height increases, total horizontal aeolian sediment flux increases and explains 58% of the variation in total horizontal aeolian sediment flux. We also test a probabilistic model of wind erosion based on gap size between vegetation elements scaled by vegetation height (the Okin model), which predicts measured total horizontal aeolian sediment flux more closely than another commonly used model based on the average plant area observed in profile (Raupach model). The threshold shear velocity of bare soil appears to increase as gap size between vegetation elements scaled by vegetation height increases, reflecting either surface armoring or reduced interaction between the groundwater capillary zone and surface sediments. This work advances understanding of the importance of measuring gap size between vegetation elements scaled by vegetation height for empirically estimating Q and for structuring process-based models of desert wind erosion in groundwater-dependent vegetation.

Citation: Vest, K. R., A. J. Elmore, J. M. Kaste, G. S. Okin, and J. Li (2013), Estimating total horizontal aeolian flux within shrub-invaded groundwater-dependent meadows using empirical and mechanistic models, *J. Geophys. Res. Earth Surf.*, *118*, 1132–1146, doi:10.1002/jgrf.20048.

1. Introduction

[2] A leading challenge in aeolian geomorphology is understanding the influence of vegetation structure on total horizontal aeolian sediment flux, Q ($\mathrm{kg\,m^{-1}\,s^{-1}}$) [*Musick and Gillette*, 1990; *Musick et al*., 1996; *Wolfe and Nickling*, 1996; *Belnap and Gillette*, 1998; *Lancaster and Baas*, 1998; *Okin and Gillette*, 2001; *King et al*., 2005; *Peters et al*., 2006; *Li et al*., 2007; *Li et al*., 2009; *Okin et al*., 2009]. Because vegetation structure influences flow regimes, shear stress, and surface erodibility [*Shao*, 2000], the absence of vegetation raises the potential for increased Q [*Marshall*, 1971; *Raupach*, 1992; *Lancaster and Baas*, 1998]. Likewise, dust emissions to the atmosphere are proportional to the horizontal flux of saltating grains, aerodynamic entrainment, and aggregate disintegration at the surface, with proportionality related to the structure and texture of the underlying soil [*Gillette et al*., 1997, *Shao et al*., 2011]. Therefore, land use activities that alter the cover or 3-dimensional structure of desert vegetation pose a challenge to resource managers seeking to maintain soil stability and limit air pollution. Of particular concern are land use practices that contribute to woody encroachment of grasslands [*Schlesinger et al*., 1990], destroy biological soil crusts [*Belnap*, 1995], or otherwise lead to conditions of increasing shear velocity at the soil surface.

[3] In desert systems prone to high winds and friable soils, vegetation structure must be actively managed, through either direct (e.g., seeding of grass and fire treatments) or indirect methods (e.g., modification of grazing intensity and management of groundwater depth). For management to be successful, methods are needed for predicting Q from a limited number of observations. In empirical models, these observations are used to develop statistical relationships between vegetation structure and Q, both measured in natural settings. Once constructed, empirical models might be used for quick assessment of site conditions and for

[1]Appalachian Laboratory University of Maryland Center for Environmental Science, Frostburg, Maryland, USA.
[2]Department of Geology, The College of William and Mary, Williamsburg, Virginia, USA.
[3]Department of Geography, University of California Los Angeles, Los Angeles California, USA.

Corresponding author: K. Vest, University of Maryland Center for Environmental Science, Appalachian Laboratory, 301 Braddock Rd, Frostburg, MD 21532, USA. (kvest@umces.edu)

2169-9003/13/10.1002/jgrf.20048

estimating the potential for future erosion. Careful use of process-based models, on the other hand, requires observations of both soil and vegetation properties but has the potential to reveal how these properties influence Q. Here, the choice of how to represent vegetation structure and distribution can be informed by empirical models as the choice appears in part to determine model success.

[4] Parameters that quantify the average profile area of vegetation (per unit ground area) encountered by the wind (e.g., "lateral cover" [*Marshall*, 1971; *Raupach*, 1992; *Raupach et al*., 1993; *Marticorena and Bergametti*, 1995; *Musick et al*., 1996; *Wolfe and Nickling*, 1996; *Marticorena et al*., 1997; *Dong et al*., 2001]) have long been considered useful for estimating the shear velocity at the soil surface. Although there is evidence that the configuration of vegetation and other roughness elements has a limited impact on wind erosion [*Brown et al*., 2008], recent work suggests otherwise. The spatial distribution of vegetation elements (e.g., vegetation clumping and connectivity of bare soil patches) is expected to have a strong effect on wind erosion, reflecting the fact that shear velocity is spatially variable across a vegetated surface [*Okin*, 2008; *Okin et al*., 2009]. *Okin* [2008] compared the theoretical underpinnings of the Raupach model [1993] (based on lateral cover) to a new model that uses scaled gap size ($\bar{L}/h$, average gap size divided by average vegetation height) to represent vegetation structure. By representing bare soil surfaces as a probabilistic distribution of gaps of a certain size, *Okin* [2008] suggested that Q is more sensitive to vegetation structure and distribution than to vegetation (lateral) cover [see also *Okin et al*., 2006]. However, the Okin model has yet to be tested in a variety of settings using field observations collected for this purpose.

[5] In this paper, we evaluated a suite of vegetation parameters identified from the literature [*Marshall*, 1971; *Okin*, 2008; *Breshears et al*., 2009] including those described above, for their capability to explain variability in Q across a shrubland to grassland gradient within groundwater-dependent vegetation in the Owens Valley, California. Although extensive work has explored dust emission from Owens dry lake [*Goudie and Middleton*, 1992; *Cahill et al*., 1996; *Gill*, 1996; *Reheis*, 1997, 2006; *Gillette et al*., 2001], to the best of our knowledge, this study is the first to measure and analyze Q in vegetated portions of the valley to the north of the exposed lake bed (Figure 1). Vegetation cover and

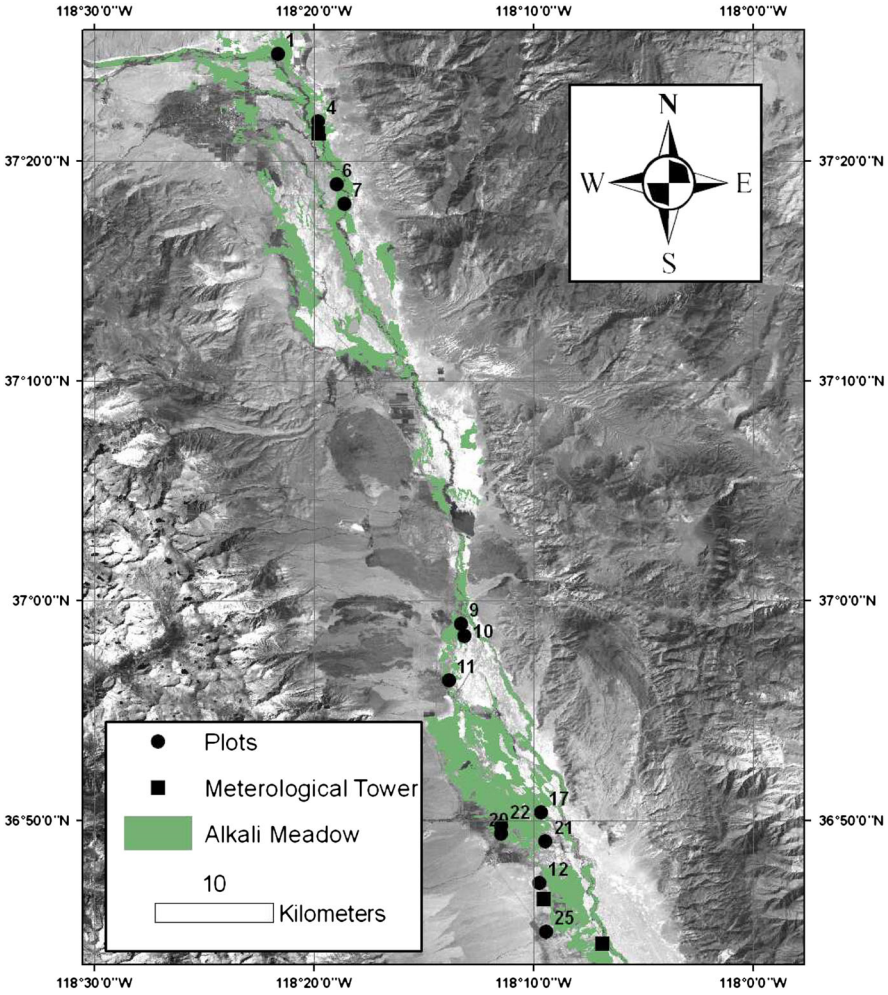

Figure 1. The plots where BSNE stems were installed across the Owens Valley in alkali meadow identified using the vegetation survey of 1986 [*James et al*., 1990]. There are two meterological towers located in the southern half of the valley and one located in the north (squares). The background is a Landsat TM image from 8 September 1992.

structure in Owens Valley has been adversely affected by groundwater pumping over the past several decades [*Elmore et al*., 2003, 2006, 2008]. *Mata-Gonzalez et al*. [2012] looked at microtopograpic effects, which can be created by wind or water erosion. The finding that shrubs are more often located on relatively high locations is consistent with the idea that shrubs trap sediment carried by wind from bare soil areas. Today, groundwater pumping is actively managed using, to some extent, observations of change in vegetation structure, making this a useful study system for developing tools that model Q across vegetation gradients that correlate with groundwater depth and history. Further, the importance of groundwater-dependent systems as sources of atmospheric dust emission has recently been highlighted [*Reynolds et al*., 2007], adding additional motivation for understanding these systems. We intend the results of this work to lend insight into future model development and testing as well as into the development of sustainable management plans.

2. Methods

2.1. Study Site

[6] Owens Valley is a semiarid endorheic basin in California situated between the Sierra Nevada and the White-Inyo mountain ranges, receiving a median precipitation of 0.13 m annually. Snowmelt from the Sierra Nevada results in $5.8 \times 10^8\,m^3$–$6.3 \times 10^8\,m^3$ annual runoff that recharges groundwater and surface water in the Owens River drainage basin. Originally, these waters flowed to the Owens Lake located at the southern terminus of the Owens River Basin [*Hollett et al*., 1991; *Danskin*, 1998]. Due to annual recharge, the groundwater table is close to the surface across much of the Owens Valley floor supporting the shallow-rooted alkali meadow vegetation community [*Sorenson et al*., 1991; *Elmore et al*., 2003, 2006]. Saltgrass (*Distichlis spicata* (L.) Greene) and alkali sacaton (*Sporobulus airoides* Torr.) are characteristic grass species of alkali meadow and form dense grasslands in areas where the water table is within 1.5 m of the soil surface [*Sorenson et al*., 1991]. Alkali meadow also contains shrub species, such as greasewood (*Sarcobatus vermiculatus*), Nevada saltbush (*Atriplex lentiformis* ssp. *torreyi*), and rubber rabbitbush (*Ericameria nauseosa*), which occur in areas with deeper, but still accessible, groundwater [*Sorenson et al*., 1991].

[7] In 1913, the city of Los Angeles (LA) built the LA Aqueduct and diverted the Owens River contributing to the complete desiccation of Owens Lake around 1920. Subsequent dust storms in Owens Valley lead to non-compliance with National Ambient Air Quality Standards (NAAQS) for airborne particulate matter (PM_{10}) [*Reheis et al*., 2009]. Although restoration work on Owens Lake has begun to mitigate dust emissions, (document available from the U.S. Environmental Protection Agency (http://epa.gov/region09/air/owens/pmplan.html#52507)), increasing pressure on groundwater resources in the northern portions of the valley has led to the drying of springs and seeps [*Danskin*, 1998] and changes in regional vegetation [*Elmore et al*., 2003]. In particular, during the California drought from 1987 to 1992, LA increased groundwater pumping, lowering the water table below the root zone of alkali meadows in much of the valley, causing the decline of grass cover, shrub encroachment, and exposing bare soil areas [*Elmore et al*., 2006, 2008]. Due to fluctuations in groundwater depth in some areas (but not all), the cover and spatial structure of vegetation within alkali meadow are highly variable. Although the largest source of dust emission is from Owens dry lake, the similarities between the soils (e.g., puffy salt crusts that are highly susceptible to wind erosion [*Reynolds et al*., 2007]), shallow groundwater tables, and geologic history of the Owens dry lake and alkali meadow [*Orme and Orme*, 2008] suggest that alkali meadow soils would be susceptible to wind erosion wherever bare soil is exposed [*Saint-Amand et al*., 1987].

2.2. Plot Selection

[8] Our analysis focused on 13 plots (10,000 m^2 each) that were monitored for three years: 2008, 2009, and 2010. Plot selection focused on covering a range in vegetation structure, from shrubs separated by bare soil, through shrubs separated by meadow, to continuous meadow. Based on research linking vegetation structure and groundwater [*Elmore et al*., 2003, 2006], we found it possible to use spatial and recent temporal variation in groundwater depth to capture the needed variability in vegetation structure. However, we also required that groundwater be sufficiently close to the surface to justify a characterization of "groundwater dependent" and the soil characteristics associated with shallow groundwater dominated systems (generally thought of as requiring groundwater within 5 m of the surface [*Reynolds et al*., 2007]). Although cattle grazing occurs across the entire study area, data on spatial variability in grazing intensity are unavailable, and we were forced to work under the assumption that grazing had a similar impact on vegetation structure across all plots. To enable the establishment of plots along the required gradient in vegetation structure, plots were identified that were (1) within 100 m of a long-term monitoring well with recorded groundwater depths since 1986 (measured in April of each year); (2) located within alkali meadow, as identified by a 1986 vegetation survey [*James et al*., 1990]; and (3) within soil identified as mollisol or aridisol in the Soil Survey Geographic Database (SSURGO) [*Soil Survey Staff*, 2006]. Sixteen plots were initially selected in these areas. However, in 2008, destruction of three plots by cattle that had not been removed at the time of sediment trap installation reduced the number of study plots to 13 (Figure 1). We did not re-deploy at these three sites in 2009 or 2010. At eight of the 13 plots, *Aubault* [2009] performed soil texture analyses.

2.3. Field Measurements

[9] At each plot, Q was measured using four Big Spring Number Eight (BSNE) sediment traps (Custom Products and Consulting, Big Spring, TX) placed on a 1 m pole at heights of 0.1, 0.2, 0.5, and 1 m. This arrangement will henceforth be called a BSNE stem. BSNE stems were installed for three seasons (May to September 2008, 2009, and 2010) within each plot. Although dust emission during the winter might be significant [*Saint-Amand et al*., 1987], we avoided this season due to the pervasive presence of cattle over-wintering across most of the Owens Valley floor. During the summer, cattle are typically moved to higher elevation grazing lands. Although cattle likely influence vegetation structure, we know from previous research that groundwater decline is the main source of vegetation structure change [*Elmore et al*., 2003]. Also, we do not believe that cattle changed the vegetation structure considerably during the study period because the

mean vegetation structure at each plot was not significantly different across years, and we saw no evidence that there was between-plot variation in grazing intensity to the degree that it influenced vegetation structure at one plot more than another. In 2008, we placed a BSNE stem at each plot in a location characterized by either grass or a bare soil. In 2008 and 2009, we did not find differences in the amount of sediment collected between grass and bare soil locations (suggesting low within-plot variability in Q and sediment sources from outside the immediate vicinity of the BSNE stem). Therefore, in 2010, we placed all BSNE stems in bare soil locations. The reason the location did not effect the sediment collected was because the sediment in each of the traps was from a wider area than where the BSNE stem was placed. The average diameter of bare soil around the BSNE stems was approximately 3.16 m in 2008, 4.41 m in 2009, and 5.23 m in 2010. In 2009 and 2010, two BSNE stems were placed at two of the plots to explore spatial variation in Q, and tiles were placed around the BSNE stem at each plot to prevent vegetation growth around the lowest trap that might prevent trap movement and obstruct the inlet (something that occurred at plots 1, 4, 7, 10, 20, and 25 in 2008). BSNE stems were not placed within 1 m of shrubs. The height of each trap was measured from the ground surface to the bottom of the inlet. The mass of the sample collected in each trap was divided by sampler inlet area and the duration of collection time, $q(z)$ ($\mathrm{kg\,m^{-2}\,s^{-1}}$). The results from each trap were fit to an exponential equation that was integrated from the ground surface to 1 m to estimate Q ($\mathrm{kg\,m^{-1}\,s^{-1}}$) [*Shao and Raupach*, 1992; *Gillette*, 1997]. The Q was adjusted to account for the known efficiency of the BSNE stem, 90% ± 5% [*Shao et al*., 1993].

[10] Vegetation cover, gap distribution, and vegetation height for each plot were determined using four 50 m line intercept transects run in cardinal directions from the BSNE stem [*USDA and NRCS*, 2004]. For each transect, along-transect width (greater than 0.03 m), species, height of vegetation (greater than 0.08 m), and along-transect width of bare soil patches (greater than 0.03 m) were measured. Despite the imposed detection limit in vegetation height, we found that even the shortest vegetation elements were taller than 0.08 m. The vegetation height was measured using a regulation Frisbee® with a hole carved into the center through which a wooden meter stick could be threaded. The meter stick was placed in each individual plant along the transect, and the Frisbee® was dropped vertically with the meter stick penetrating the hole in the disk. The top of the plastic disk at its stopping location was recorded as the vegetation height. Vegetation transects were conducted in May of 2008, 2009, and 2010 during BSNE stem deployment.

[11] Meteorological data were measured at three locations across Owens Valley (Figure 1). Wind velocities were measured in 2009 and 2010 using five tower-mounted anemometers positioned above the ground at 0.5, 1, 2, 5, and 10 m (wind velocity height used to estimate U). In 2008 at the two southern towers, wind velocity was only measured at 10 m. Average wind velocities were recorded every 10 min on the two southern towers and every 5 min on the northern tower. Data from an air temperature and humidity sensor mounted at 2 m were collected every 3 s and averaged at 10 min intervals at the two most southern towers. These measurements were collected over the duration of each sampling period in 2008, 2009, and 2010. Precipitation measurements were collected by the Los Angeles Department of Water and Power and the Inyo County Water Department at rain gauges across Owens Valley.

[12] Threshold shear velocity (u_{*_t}) is the minimum shear velocity that generates the force required to begin moving particles on bare soil generating Q (Table 1) [*Belnap and Gillette*, 1998]. When shear velocity is less than u_{*_t}, there is no sediment movement. u_{*_t} can be measured directly using a wind tunnel (this method is expensive and logistically difficult [*Li et al*., 2009]) or by using a particle sensor attached to a tower fitted with anemometers [*Lancaster and Baas*, 1998]. We were not able to use either of these methods at our plots; therefore, we estimated u_{*_t} using (1) a relationship between soil texture and u_{*_t} identified from the literature [*Gillette et al*., 1980, 1982; *Cahill et al*., 1996; *Gillette and Passi*, 1988], and (2) a relationship between surface strength and u_{*_t} [*Li et al*., 2010].

[13] The threshold shear velocity of bare soil ($u_{*_t\mathrm{field}}$) was estimated by firing a spherical copper pellet (0.0045 m diameter BB) into the bare soil surface at 45° using a 760 Pumpmaster air gun with a muzzle height of 0.15 m (following methods described by *Li et al*. [2010]). For each plot, a 50 m tape was run in a cardinal direction from the BSNE stem, and a BB was shot every 5 m. The BB holes were typically elliptical, and the area of the hole ($\mathrm{m^2}$) was calculated using the maximum diameter and a line perpendicular to the maximum diameter. In addition, a pocket penetrometer (QA Supplies, FT011) applied at 45° to the soil surface was used to measure the resistance of the soil surface [*Li et al*., 2010]. Working with desert soils at lands near Moab in SE Utah, *Li et al*. [2010] calculated $u_{*_t\mathrm{field}}$ using a linear relationship with the area of the hole produced by the BB (BB; *Li et al*. [2010] uses $\mathrm{BB_{area}}$) and the force for the penetrometer to puncture the soil surface (F; *Li et al*. [2010] uses *Penetrometer*), and $u_{*_t\mathrm{field}}$ (Table 1).

$$u_{*_t\,\mathrm{field}} = 10^{4.095-(0.078*\mathrm{BB})+(0.191*F)} \quad (1)$$

[14] We used this method and applied equation (1) to soils at our plots in 2009. Although there might have been changes in u_{*_t} annually, there were no detectable differences in depth to water, gap size, or vegetation structure. Therefore, we do not find it likely that u_{*_t} changed across the three study years.

2.4. Remote Sensing of Vegetation Cover

[15] We acquired Landsat ETM+ images in September 2008, 2009, and 2010 to estimate the fraction of photosynthetic vegetation (%PV) at each site using linear spectral mixture analysis [*Elmore et al*., 2000]. These data were previously validated against field measurements of leaf area along 33 permanent transects and found to be accurate to within ±4.0% PV (absolute percent cover units) and are therefore useful for a variety of land use and land cover change investigations [*Elmore et al*., 2003, 2006]. We sampled %PV cover at each plot from these raster data sets and calculated three different %PV statistics: single pixel, nine-pixel mean, and the standard deviation of the nine pixels, at and around each plot.

Table 1. Description of Parameters Used in the Paper

Parameter	Equations	Description	Units
A	6 and 10	This is a constant equal to 1 that accounts for relative availability of sand particles for transport.	Unitless
A_B	2 and 9	This is the average basal area of the plants from transect data.	m^2
A_P	2 and 9	This is the average profile area of plants from transect data.	m^2
β	8, 9, and 10	This is the ratio of element to surface drag coefficients (~100).	Unitless
C	9 and 10	This is the percent vegetation cover of an area.	%
$\%C$	Not applicable	The percentage of the total amount of roughness elements in an area.	%
C_r	Not applicable	This is the concentration of roughness elements.	Unitless
D	5	This is the displacement height from the ground to the anemometer.	m
F_g	3	This is the fraction of bare ground.	Unitless
g	6 and 10	This is the acceleration due to gravity.	$m\,s^{-2}$
κ	5	The Kármán constant is used to describe the logarithmic velocity profile of wind velocity near a boundary.	Unitless
$\bar{L}$	2 and 11	This is the average gap size length from transect data.	m
$\bar{L}/h$	11	This is the scaled gap size.	Unitless
λ	2 and 8	This is the canopy cover as viewed from the side (most commonly used parameter to define vegetation structure in wind erosion models).	Unitless
m	8	This has the value of 1 for surfaces that are topographically stable.	Unitless
$P_d(x/h)$	3	This is the probability that any point is a distance, x, from the nearest upwind plant of height, h.	Unitless
$P_d{}^U(x/h)$	7	This is the probability that any point is a certain distance, x/h, at wind speed U.	Unitless
$q(z)$	Not applicable	The mass of the sample collected in each trap divided by sampler inlet area and the duration of collection time.	$kg\,m^{-2}\,s^{-1}$
Q	7, 10, and 11	This is the total horizontal flux.	$kg\,m^{-1}\,s^{-1}$
Q^U	3 and 7	This is the total horizontal flux at a certain wind speed U.	$kg\,m^{-1}\,s^{-1}$
$Q^U_{(x/h)}$	3 and 6	This is the horizontal flux for any points a distance x/h from the nearest upwind plant.	$kg\,m^{-1}\,s^{-1}$
ρ	6 and 10	This is the air density.	$kg\,m^{-3}$
σ	8	This is the ratio of the basal area to the frontal area of the vegetation. $\sigma = \frac{A_B}{A_P}$	Unitless
$U(z)$	5	This is the wind speed at height (z).	$m\,s^{-1}$
u_*	4, 5, 6, 8, and 10	This is the surface shear velocity.	$m\,s^{-1}$
u_{*_s}	6	This is the surface shear velocity in presence of vegetation	$m\,s^{-1}$
$\left(\frac{u_{ss}}{u_*}\right)$	4	Ratio of shear velocity in the presence of plants to shear velocity in the absence of plants	Unitless
u_{*_t}	6, 8, 9, and 10	Threshold shear velocity of bare soil is the shear speed at which particles on bare soil begin to move generating particle movement.	$m\,s^{-1}$
$u_{*_t\text{field}}$	1	Threshold shear velocity (u_{*_t}) estimated from penetrometer and BB-hole measurements.	$m\,s^{-1}$
$\overline{W}$	2	The average plant width from transect data.	m
%WC	Not applicable	The percent of the fraction of ground covered by woody perennial plants, live and dead.	%
z_0	5	This is the roughness height.	m

2.5. Field-Measured Parameters

[16] We evaluated the capability of six different vegetation parameters to explain variation in Q: lateral cover (λ) (1.3×10^{-5} to 0.18), concentration of roughness elements (C_r) (4.7×10^{-2} to 11), percent cover of woody vegetation ($\%W_c$) (6.1% to 79%), percent cover ($\%C$) (23% to 96%), average gap size ($\bar{L}$) (0.20 m to 3.9 m), and scaled gap size ($\bar{L}/h$) (1.8 to 10) (Table 1). All vegetation parameters were chosen from literature and were calculated from the described field observations.

[17] Lateral cover (λ) was chosen as a parameter because it has been used to define vegetation structure in wind erosion research since *Marshall* [1971]. λ is the plant area observed in profile encountered by the wind as it flows over the surface. Due to the difficulty of calculating a true lateral cover parameter from transect data, we used an equation from *Okin* [2008] that relates lateral cover to average gap size ($\bar{L}$) with the following formula:

$$\lambda = \frac{A_P \overline{W}}{A_B(\bar{L} + \overline{W})}, \tag{2}$$

where A_P is profile area of the plant, A_B is the basal area, $\overline{W}$ is the average plant width, and $\bar{L}$ is the average gap size. We calculated A_P assuming plant profiles resemble an ellipse defined by plant height and plant diameter along the transect, which we measured in the field. The basal area was estimated by assuming plants resemble a circle (as viewed from above) with a radius equal to half the shrub diameter.

[18] Percent woody cover ($\%W_c$) was chosen for two reasons: (1) variation in woody vegetation amount and density was immediately apparent across our plots, and (2) shrublands generally exhibit elevated Q over grasslands [*Breshears et al.*, 2009]. $\%W_c$ was calculated as the fraction of ground covered by the characteristic shrub species, live and dead.

[19] *Fryrear* [1985] found that any type of roughness element (e.g., soil clods and plant litter) decreased wind erosion on bare soil. Therefore, we chose to use the vegetation parameter percent cover ($\%C$) to represent the total amount of roughness elements in an area. $\%C$ was estimated by calculating the percentage of vegetation and litter covering all transects compared to bare soil area.

[20] The aforementioned vegetation parameters focused primarily on quantifying the vegetation amount ($\%W_c$ and $\%C$) and arrangement in the landscape (λ and C_r). However, bare soil is the erodible substrate; therefore, the following parameters focus on estimating the area of susceptible bare soil to wind erosion: average gap size ($\bar{L}$) and gap size scaled

by vegetation height $(\bar{L})/h$. $\bar{L}$ is calculated as the average distance between shrubs and grass plants along transects. $\bar{L}/h$, where h is the average plant height in transects, accounts for the fact that the length of the wake downwind of a plant depends upon the plant height [*Okin*, 2008].

2.6. Statistical Analysis

[21] Using an ANOVA with Tukey Honestly Significant Difference (HSD), we examined whether there were differences between Q and vegetation parameters collected annually over the three-year period. We then used an ANOVA with Tukey HSD to examine the differences in the means of relative humidity (a higher relative humidity increases u_{*_t} which decreases dust emission [*Nickling and Neuman*, 1997; *Park and In*, 2003]), wind velocity, and temperature to try and explain any observed differences. Using linear and rank regression, we examined the relative capability of each parameter (derived from remote sensing, vegetation, or gap measurements) to explain the variability between plots and years in the measured Q. To determine the most explanatory model for Q using any combination of vegetation parameters, all the parameters were linearly regressed against Q using all possible regressions, step-wise regression, forward entry regression, and backward regression, using a P value cutoff of 0.01.

2.7. Process-Based Modeling: The Okin Model

[22] The goal of wind erosion models is to calculate total horizontal sediment flux (Q) from a limited set of lab and field-measured parameters. A principal challenge in modeling wind erosion on vegetated landscapes is the choice of a vegetation distribution parameter that does not describe shear stress on the surface as homogeneous [*Okin*, 2005, 2008]. Since 1971, vegetation measurements for wind erosion models have used lateral cover (λ) [*Marshall*, 1971; *Raupach et al*., 1993; *Okin*, 2008]. Yet, λ (i.e., plant area observed in profile) is an imperfect representation of vegetation cover because a few tall plants are treated equally to a greater number of short plants, and field observations demonstrate that Q can be dependent on vegetation distribution [*Gillette et al*., 2006; *Okin*, 2008]. Furthermore, λ is difficult to calculate because both the frontal silhouette area of vegetation and average footprint per plant are required measurements [*Marshall*, 1971; *Okin*, 2008]. The Okin model, on the other hand, uses the full probability distribution of gap sizes scaled by vegetation height as measured in the field [*Okin*, 2008].

[23] The model itself is described in detail by *Okin* [2008]. Briefly, Q^U (total horizontal flux at a certain wind velocity U) is modeled using the distribution of gaps downwind of the nearest upwind plants as

$$Q^U = F_g \int_0^\infty Q^U_{x/h} P_d(x/h)\, d(x/h), \tag{3}$$

where $P_d(x/h)$ is the probability that any point is a distance, x, downwind of vegetation of height, h; F_g is the fraction of bare ground; and $Q^U{}_{(x/h)}$ is the horizontal flux associated with bare soil at the x/h position.

[24] The reduction in shear velocity associated with a plant spacing of x/h is described by an exponential curve as follows:

$$\frac{u_{*_s}}{u_*} = \left(\frac{u_{*_s}}{u_*}\right)_{x=0} + \left[1 - \left(\frac{u_{*_s}}{u_*}\right)_{x=0}\right] * \left[1 - e^{-xc_1/h}\right], \tag{4}$$

where u_{*_s}/u_* is the ratio of shear velocity in the presence of plants (u_{*_s}) to the shear velocity in the absence of vegetation (u_*), $(u_{*_s}/u_*)_{x=0}$ is the depressed shear velocity in the immediate lee of a plant, and c_1 is the e-folding length expressed in units of height (4.8) [*Okin*, 2008]. We studied the literature [*King et al*., 2005] and compared the description of vegetation type and associated values for $(u_{*_s}/u_*)_{x=0}$ with vegetation at our plots. From this analysis, we arrived at the value of 0.2 for $(u_{*_s}/u_*)_{x=0}$. We then calculated u_* (i.e., the law of the wall [see *Priestley*, 1959]) as

$$u_* = \frac{U(z)\kappa}{\mathrm{In}((z-D)/z_0)}, \tag{5}$$

where $U(z)$ ($\mathrm{m\,s^{-1}}$) is the wind velocity at height z (m) measured at each tower, $\kappa = 0.4$, D is the displacement height (i.e., 0 so that wind erosion is allowed on vegetated surfaces), and z_0 is the roughness height of bare soil (m) (0.001). In many wind erosion models, z_0 is the roughness height that varies over heterogeneous surfaces related to both plant cover and canopy height. However, in the Okin model, z_0 is the roughness height of bare soil between plants and is considered to be independent of plant parameters. We assume that z_0 defined in this way is the same for all plots. We chose the value because it was the average estimate between the roughness height of bare soil (0.0001 m to 0.0008 m) in arid and semiarid regions using an ERS scattermeter [*Prigent et al*., 2005] and the roughness height of biological crusts ((0.0006 m to 0.0137 m) in Table 1 of *Rodriquez-Caballero et al*. [2012]). We did not independently measure a roughness height ourselves, and we acknowledge that the roughness exhibited by soils will lead to differences n z_0. We also assume that the variance in roughness length due to soil roughness (z_0) is small compared to that imposed by vegetation structure and therefore use the same z_0 for all plots.

[25] Flux at any plant spacing, $Q^U{}_{(x/h)}$, was calculated by using the formulation by *Shao et al*. [1993] later modified to include the distance (x/h) from the nearest upwind plant:

$$Q^U_{(x/h)} = A\frac{\rho}{g} u_* \left(u_*^2 - u_{*t}^2\right)\delta, \tag{6}$$

where A is a constant equal to one that accounts for the relative availability of sand particles for transport [*Gillette et al*., 2001], ρ is air density at 23.3 °C and 1400 m (average temperature over BSNE deployment for three years and average elevation of Owens Valley; $1.01\,\mathrm{kg\,m^{-3}}$), g is acceleration due to gravity ($9.8\,\mathrm{m\,s^{-2}}$), u_* is the surface shear velocity, u_{*_t} is the threshold shear velocity of bare soil, and δ is set to 0 when $(u_{*_t} > u_*)$ and 1 otherwise. The units of $Q^U{}_{(x/h)}$ are horizontal mass flux ($\mathrm{kg\,m^{-1}\,s^{-1}}$). Finally, Q for all wind velocities were calculated by

$$Q = \int_0^\infty P_d^U Q^U d(U) \tag{7}$$

which integrates Q^U over the full probability distribution of measured wind velocities $P_d{}^U$.

2.8. Mechanistic Modeling: The Raupach Model

[26] The Raupach model calculates threshold shear velocity by using the parameter λ (i.e., plant area observed in profile) [*Raupach et al.*, 1993].

$$u_* = u_{*_t}\sqrt{(1 - m\sigma\lambda)(1 + m\beta\lambda)}, \quad (8)$$

where u_* is the threshold shear velocity in the presence of vegetation and u_{*_t} is the threshold shear velocity of the bare soil surface. β is the ratio of the drag coefficient of a single element divided by the drag coefficient of the bare ground. $\beta = 100$ and $m = 1$ because these are the values recommended by *Raupach et al.* [1993] for flat erodible surfaces. σ is the ratio of the basal area to the frontal area of the vegetation, $\sigma = \frac{A_B}{A_P}$ (Table 1) [*Okin*, 2008].

[27] To incorporate the relationship between λ and percent vegetation cover, C, the Raupach model can be re-expressed as

$$u_{*_t} = u_*\sqrt{(1 - C)\left(1 + \beta C\frac{A_P}{A_B}\right)} \quad (9)$$

[28] The terms $(1 - m\sigma\lambda)$ in equation (8) and $(1 - C)$ in equation (9) each account for vegetation covering part of the surface, thus resulting in greater shear stress on the remaining bare ground [*Okin*, 2005]. The terms $(1 + m\beta\lambda)$ in equation (8) and $\left(1 + \beta C\frac{A_P}{A_B}\right)$ in equation (9) account for the partition of some of the shear stress onto the vegetation and away from the soil surface.

[29] By combining equations (6) and (9) and using the $u_{*_t\text{field}}$, we solved for Q_{Raupach} as follows:

$$Q_{\text{Raupach}} = A\frac{\rho}{g}u_*\left(u_*^2 - \left(u_{*_t}\sqrt{(1 - C)\left(1 + \beta C\frac{A_P}{A_B}\right)}\right)^2\right) \quad (10)$$

2.9. Model Comparison

[30] We used the Okin model to calculate the total horizontal aeolian sediment flux at each plot using a uniform u_{*_t} ($0.56\,\text{m s}^{-1}$) (Q_{Uniform}) and a u_{*_t} estimated using data collected separately at each plot (Q_{Okin}) (Table 2). The uniform u_{*_t} value was chosen based on published values (Table 3), suggesting that a u_{*_t} of $0.56\,\text{m s}^{-1}$ was an appropriate average value for alkali meadow in Owens Valley. We compared modeling results to measured Q (Q_{field}) (Table 2) from the deployed BSNE stems by using a nonparametric ANOVA. We measured u_{*_t} at each plot separately using equation (1) and recalculated Q using the Okin model (QOkin). We also calculated Q using the Raupach model (QRaupach) for each plot, using u_{*_t} field. To determine whether the Okin model predicts Q better than the Raupach model at our plots, a nonparametric ANOVA was performed in R between the QOkin, QRaupach, and Qfield. In all statistical analyses, we used a critical P value of 0.01 to determine significance.

3. Results

3.1. Comparing 2008, 2009, and 2010 Data

[31] The seven different vegetation parameters (Table 4) were similar in 2008, 2009, and 2010 (ANOVA with Tukey HSD) except for $\%W_c$, which was significantly different between the years 2008 and 2010 ($P = 0.003$) and 2009 and 2010 ($P = 0.002$). The Q_{field} was also significantly different between the years 2008 and 2010 ($P < 0.001$) and 2009 and 2010 ($P < 0.001$) (ANOVA with Tukey HSD), but the Q_{field} in 2008 and 2009 was not significantly different ($P = 0.99$). This led us to run ANOVAs with Tukey HSD between wind velocities, depth to water (DTW), relative humidity, and temperature for these three different years. We also compared precipitation during BSNE deployment for the three-year period. The mean wind velocities in 2009 and 2008 were not significantly different ($P = 0.74$); however, the mean wind velocities in 2008 and 2010 ($P < 0.001$) and 2009 and 2010 ($P < 0.001$) were significantly different, with a higher average wind velocity in 2010. During the duration of BSNE stem deployment in 2010, 4.6% of days exhibited wind velocities greater than $10\,\text{m s}^{-1}$ (at 10 m height) compared to 3.50% and 1.40% in 2008 and 2009, respectively, indicating that the wind velocity distribution was more skewed toward higher values in 2010. The means of DTW between 2008, 2009, and 2010 were not significantly different ($P = 0.81$). The means between relative humidity were different between 2008 and 2009 ($P < 0.001$) and 2009 and 2010 ($P < 0.001$) but indistinguishable between 2008 and 2010 ($P = 0.54$); however, the number of days with relative humidity greater than 60% during BSNE stem deployment in 2010 was <1% compared to 3.5% and 1.40% for 2008 and 2009, respectively. Mean temperature between 2010 and 2009, and 2010 and 2008 were significantly different with temperatures being colder in 2010 ($P < 0.001$ for both). *Reynolds et al.* [2007] note that dust emission suppression only occurs during heavy rainfall, but the largest average event in Owens Valley was only 0.003 m during BSNE deployment in 2008. Although 2010 had the lowest amount of precipitation during BSNE deployment of the three years, we do not believe that rainfall influenced changes in Q greatly. Therefore, compared with 2008 and 2009, the summer of 2010 exhibited a higher average wind velocity, greater number of days with high winds, low humidity, and on average colder temperatures.

3.2. Empirical Relationship Between Q_{field} and Vegetation

[32] We combined the field measurements (Q_{field} and each vegetation parameter) for all years (i.e., 2008, 2009, and 2010) and analyzed the vegetation parameters against Q_{field}, but this did not result in any vegetation parameter explaining greater than 50% of the variation in Q_{field} using a critical P value of 0.01. Therefore, we analyzed vegetation parameters from 2008 and 2009 separately from vegetation parameters from 2010 against Q_{field} (Table 4). We felt this was justified by the differences in Q_{field} in 2010 apparently driven by drier, colder, gustier conditions. The vegetation parameters from 2008 and 2009 analyzed independently against Q_{field} only resulted in one parameter (scaled gap size, $\bar{L}/h$) explaining greater than 50% of the variation in Q_{field} (adjusted $R^2 = 0.56$; $P < 0.001$) (Table 4 and Figure 2d).

Table 2. Results of Field Data

Year	Plot	$u_{*_t\text{field}}$[a] ($m\,s^{-1}$)	L/h	% Bare Soil	Q ($kg\,m^{-1}\,s^{-1}$)	Soil Type
2008	1	0.83	1.9	5.6	2.6×10^{-9}	NM
2008	4	0.68	10	77	3.6×10^{-8}	Sandy/silty loams
2008	6	0.58	3.6	58	2.8×10^{-8}	NM
2008	7	0.36	6.0	68	2.6×10^{-8}	Loamy sands
2008	9	0.40	3.4	36	2.9×10^{-8}	Loamy sands
2008	10	0.91	5.3	54	2.6×10^{-8}	Loamy sands
2008	11	0.40	4.7	54	2.8×10^{-8}	NM
2008	12	0.51	5.0	49	3.0×10^{-8}	NM
2008	17	0.51	3.7	40	1.0×10^{-8}	Sandy/silty loams
2008	20	0.58	1.8	31	1.1×10^{-8}	Loamy sands
2008	21	0.51	3.3	48	1.9×10^{-8}	Sandy/silty loams
2008	22	0.43	2.6	11	7.0×10^{-9}	NM
2008	25	0.56	4.9	24	2.4×10^{-8}	Sandy/silty loams
2009	1	0.83	1.8	2.0	3.7×10^{-9}	NM
2009	4	0.68	6.2	58	2.9×10^{-8}	Sandy/silty loams
2009	6	0.58	3.6	59	2.4×10^{-8}	NM
2009	7	0.36	6.4	71	2.3×10^{-8}	Loamy sands
2009	9	0.40	4.0	47	2.5×10^{-8}	Loamy sands
2009	10	0.91	6.6	53	1.9×10^{-8}	Loamy sands
2009	11	0.40	5.9	58	3.4×10^{-8}	NM
2009	12[b]	0.51	4.1	35	1.9×10^{-8}	NM
2009	17	0.51	3.9	58	7.8×10^{-9}	Sandy/silty loams
2009	20	0.58	1.9	30	5.0×10^{-9}	Loamy sands
2009	21	0.51	5.2	76	9.5×10^{-9}	Sandy/silty loams
2009	22	0.43	2.4	22	1.2×10^{-8}	NM
2009	25[b]	0.56	7.6	57	3.4×10^{-8}	Sandy/silty loams
2010	1	0.83	2.4	4.0	2.8×10^{-8}	NM
2010	4	0.68	8.2	66	4.0×10^{-7}	Sandy/silty loams
2010	6	0.58	4.7	32	5.0×10^{-8}	NM
2010	7	0.36	4.9	50	1.2×10^{-7}	Loamy sands
2010	9	0.40	6.9	67	1.9×10^{-7}	Loamy sands
2010	10	0.91	7.3	72	4.2×10^{-7}	Loamy sands
2010	11	0.40	6.8	63	3.8×10^{-7}	NM
2010	12[b]	0.51	4.5	25	1.9×10^{-6}	NM
2010	17	0.51	5.3	46	2.3×10^{-7}	Sandy/silty loams
2010	20	0.58	3.3	35	4.7×10^{-8}	Loamy sands
2010	21	0.51	2.4	34	1.2×10^{-7}	Sandy/silty loams
2010	22	0.43	2.0	22	5.0×10^{-8}	NM
2010	25[b]	0.56	6.0	71	2.5×10^{-7}	Sandy/silty loams

Not measured (NM) means that texture analysis was not completed for the plot.
[a]The $u_{*_t\text{field}}$ was only measured in 2009.
[b]Plots 12 and 25 had two BSNE stems each. The u_{*_t}, L/h, % Bare Soil, and Q are an average of these two BSNE stems.

Table 3. Threshold Shear Velocity (average = $0.56\,m\,s^{-1}$)

u_{*_t} Ranges	Soil Type	Study Site	Citation
0.4–>1.54[b] $m\,s^{-1}$	Silt Loam	Lake Danby, CA	*Gillette et al*. [1980]
0.4–0.75[b] $m\,s^{-1}$	Loamy Sand	Shadow Mnt, CA	*Gillette et al*. [1980]
0.59–2.78[b] $m\,s^{-1}$	Sandy Loam	Lake Danby, CA	*Gillette et al*. [1980]
~0.3–1.8[b] $m\,s^{-1}$	Dry Lake	Owens Lake, CA	*Gillette et al*. [1982]
0.4–1.14[b] $m\,s^{-1}$	Sandy Crust	Owens Lake, CA	*Gillette et al*. [1982]
0.49–0.67[b] $m\,s^{-1}$	Coarse Sand	Owens Lake, CA	*Gillette et al*. [1982]
Smooth—0.35[b] $m\,s^{-1}$	Sandy loam	Panhandle TX and OK	*Gillette and Passi* [1988]
Rough—1.5[b] $m\,s^{-1}$			
Crusted—0.8[b] $m\,s^{-1}$			
Smooth—0.75[b] $m\,s^{-1}$	Silt loam	Panhandle TX and OK	*Gillette and Passi* [1988]
Rough—1.5[b] $m\,s^{-1}$			
Crusted—2.0[b] $m\,s^{-1}$			
Smooth—0.3[b] $m\,s^{-1}$	Loamy sand	Panhandle TX and OK	*Gillette and Passi* [1988]
Rough—1.0[b] $m\,s^{-1}$			
Crusted—0.35[b] $m\,s^{-1}$			
0.3–1.1[a] $m\,s^{-1}$	Unknown	Jornada, NM	*Cahill et al*. [1996]
0.28–0.9[a] $m\,s^{-1}$	Unknown	Yuma, AZ	*Cahill et al*. [1996]
0.37–0.56 $m\,s^{-1}$	Sandy/silty loams and loamy sands	Owens Valley, CA	Current study

Vegetated plots are indicated by [a] and undisturbed plots are indicated by [b].

Table 4. Regression Results

Vegetation	R^2: 2008 and 2009[c]	P Value: 2008 and 2009	R^2: 2010[d]	P Value: 2010
Λ	<0.001[a]	0.76	<0.001	0.44
C_r	0.26[a]	<0.01	0.33	0.02
$\%W_c$	<0.001	0.85	<0.001[a]	0.68
$\%C$	0.41	<0.001	0.03	0.26
$\bar{L}$	0.38	<0.001	0.48	<0.01
$\bar{L}/h$	0.56	<0.001	0.15	0.09
Percent live cover	0.25[a]	<0.01	0.11	0.12
Percent live cover	0.28[a,b]	<0.01	0.40[b]	0.01
Standard deviation from percent live cover	0.058	0.11	<0.001	0.83

[a]Log-transformed data.
[b]Average of nine pixels.
[c]Q is log-transformed.
[d]Q is ranked in the regressions.

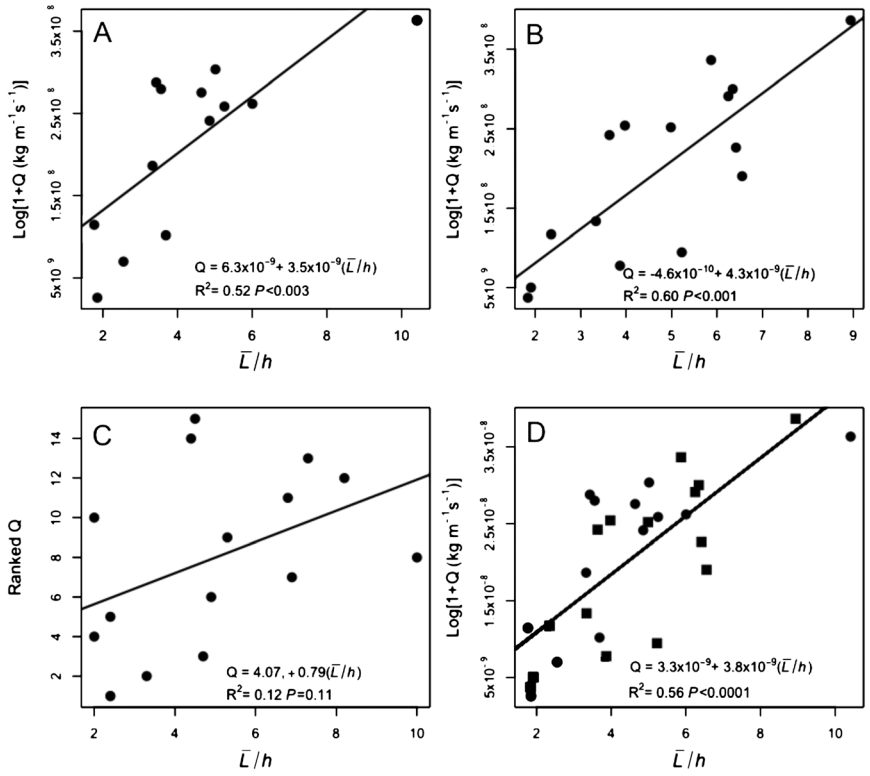

Figure 2. Scaled gap size ($\bar{L}/h$) vs. log normalized horizontal flux (Q) for 2008 (A), 2009 (B), 2010 (C), and 2008 (circles) and 2009 (blocks) combined (D). $\bar{L}/h$ in 2008 and 2009 explained 52% and 60% of the variability in Q, respectively; however, in 2010, $\bar{L}/h$ did not explain the variability in Q. Therefore, we combined the 2008 and 2009 data for our analysis and analyzed the 2010 data separately (e.g., Table 4). Together, the 2008 and 2009 data explained 56% of the variability in Q. In 2008 and 2009, lower scaled gap size results in lower Q.

The vegetation parameters from 2010 analyzed independently against Q_{field} did not result in any parameters explaining greater than 50% of the variation in Q_{field} (Table 4). The most commonly used vegetation parameter in aeolian research, λ, did not explain any variation in Q (2008 and 2009: adjusted $R^2 < 0.001$; $P = 0.76$ and 2010: adjusted $R^2 < 0.001$; $P = 0.44$) (Table 4). The combined 2008 and 2009 empirical model that explained the most variation in Q_{field} (58 %) contained the vegetation parameters, average gap size ($\bar{L}$) ($P < 0.001$), and scaled gap size ($\bar{L}/h$) ($P < 0.001$) (adjusted $R^2 = 0.58$; $P < 0.0001$), and took the following form:

$$\text{Log}(1+Q) = -2.1 \times 10^{-10} + 3.6 \times 10^{-9}(\bar{L}/h) + 2.7 \times 10^{-11}(\bar{L}) \quad (11)$$

[33] The strongest relationship between $q(z)$ (i.e., the sediment amount in the BSNE stem trap at each height divided by deployment time) and $\bar{L}/h$ was found at traps

set at 0.2 m and 0.1 m (the lowest traps), with an adjusted $R^2 = 0.54$ ($P < 0.0001$) and 0.50 ($P < 0.0001$), respectively (Figure 3). As the heights of the traps increase, the relationship between $q(z)$ and $\bar{L}/h$ decreased to an adjusted $R^2 = 0.36$ ($P < 0.001$) at 0.5 m and an adjusted $R^2 = 0.19$ ($P = 0.01$) at 1 m (Figure 2). For 2010 data, $\bar{L}/h$ at 0.1 m and 0.2 m explained less variation in $q(z)$ than in 2008 and 2009 with an adjusted $R^2 = 0.23$ ($P = 0.04$) and an adjusted $R^2 = 0.14$ ($P = 0.01$). For 0.5 m and 1 m heights in 2010, $\bar{L}/h$ was an insignificant explanatory variable at a height of 0.5 m (adjusted $R^2 = 0.02$; $P = 0.29$) but became significant again at a height of 1 m (adjusted $R^2 = 0.38$; $P = 0.01$).

3.3. Model Results

[34] The means of Q_{Uniform} and Q_{field} were significantly different ($P < 0.001$). Q_{Uniform} resulted in an overestimate at a majority of plots, but one plot (plot 12 in 2010) exhibited an underestimate (Table 5). Eighteen plots had Q_{Uniform} (Table 5) values that were greatly overestimated (Table 5). These plots had a larger average $\bar{L}/h$ value than other plots (Tables 2 and 5).

[35] Mean Q_{Okin} and mean Q_{field} were not significantly different ($P = 0.02$) (Table 5). However, the Okin model seemed to overestimate Q for plots located in the mid-valley (plots 7, 9, and 11). The overestimate of Q in the mid-valley might be mechanistically related to strong cross-valley winds [*Raab and Mayr*, 2008], which could lead to soil armoring in larger gaps (i.e., an elevated u_{*_t}). Mean Q_{field}, and mean Q_{Raupach}, differed ($P = 0.005$), and the means were also different between Q_{Okin} and Q_{Raupach} ($P < 0.001$). Minimum values for Q_{Raupach} and Q_{Okin} were $0\ \text{g m}^{-1}\ \text{s}^{-1}$; these values were less than the minimum Q_{field} value of $2.59 \times 10^{-9}\ \text{g m}^{-1}\ \text{s}^{-1}$. Maximum values for Q_{Raupach} and Q_{Okin} were $1.03 \times 10^{-8}\ \text{g m}^{-1}\ \text{s}^{-1}$ and $1.69 \times 10^{-5}\ \text{g m}^{-1}\ \text{s}^{-1}$, respectively. The maximum value for Q_{field} was $1.94 \times 10^{-6}\ \text{g m}^{-1}\ \text{s}^{-1}$, thus closer to the Q_{Okin} maximum value. Plot by plot, Q_{Raupach}, values were generally less than Q_{field} values.

[36] To explore the behavior of Q_{Okin} with increasing $\bar{L}/h$, we ran the Okin model using some hypothetical parameter sets. We held % bare soil constant at an average value of 64% and varied u_{*_t} from $0.2\ \text{m s}^{-1}$ to $0.6\ \text{m s}^{-1}$ while also varying $\bar{L}/h$ across the range measured at our plots (1.9 to 10). Results of this exercise demonstrated the non-linear behavior of Q with increasing $\bar{L}/h$ (Figure 4). A linear relationship between Q and $\bar{L}/h$ (such as seen in Figures 2d and 4) crosses successive lines of constant u_{*_t}. Across a larger range in $\bar{L}/h$ than measured at our plots, we observed that if u_{*_t} is held constant at $0.56\ \text{m s}^{-1}$, Q increases exponentially until $\bar{L}/h$ equals 20 at which point, Q increases at a decreasing rate.

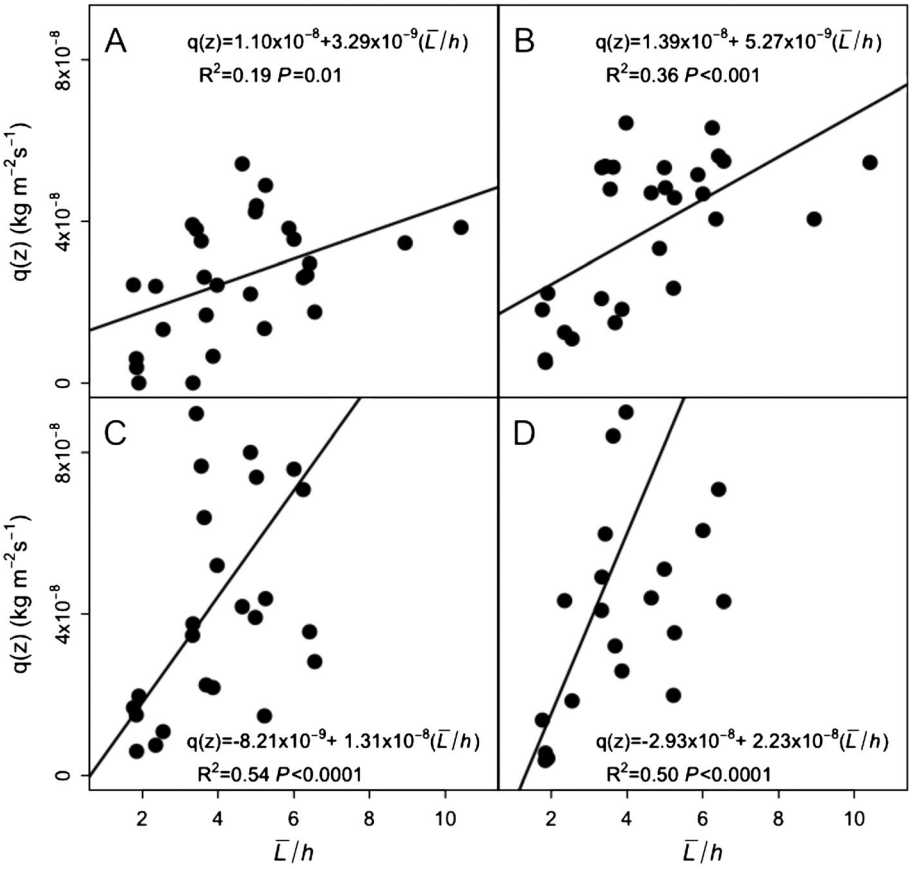

Figure 3. The effect of scaled gap size ($\bar{L}/h$) on the amount of sediment collected by BSNE stems across plots in 2008 and 2009 increased with decreasing BSNE height (A–D). The scaled gap size ($\bar{L}/h$) explains more variability in $q(z)$ at 0.2 m (C) and 0.1 m (D) than at 0.5 m (B) and 1 m (A). All results are normalized by duration of sampling time.

Table 5. Comparison Between $Q_{Uniform}$, Q_{Okin}, Q_{field}, and $Q_{Raupach}$, and ANOVA Results

Year	Plot	$Q_{Uniform}$ (kg m^{-1} s^{-1})	Q_{Field} (kg m^{-1} s^{-1})	Q_{Diff} (kg m^{-1} s^{-1})	Q_{Okin}[b] (kg m^{-1} s^{-1})	$Q_{Raupach}$[b] (kg m^{-1} s^{-1})
2008	1	2.2×10^{-7}	2.6×10^{-9}	2.1×10^{-7}	0.00	0.00
2008	4	5.8×10^{-7}	3.6×10^{-8}	5.4×10^{-7}	1.5×10^{-8}	3.1×10^{-10}
2008	6	1.4×10^{-6}	2.8×10^{-8}	1.4×10^{-6}	9.0×10^{-7}	1.6×10^{-9}
2008	7	7.9×10^{-7}	2.6×10^{-8}	7.6×10^{-7}	1.7×10^{-5}	9.2×10^{-9}
2008	9	1.0×10^{-6}	2.9×10^{-8}	1.0×10^{-6}	1.3×10^{-5}	7.3×10^{-9}
2008	10	6.5×10^{-7}	2.6×10^{-8}	6.5×10^{-7}	0.00	0.00
2008	11	1.2×10^{-6}	2.8×10^{-8}	1.2×10^{-6}	1.5×10^{-5}	7.2×10^{-9}
2008	12	1.0×10^{-6}	3.0×10^{-8}	1.0×10^{-6}	2.6×10^{-6}	3.6×10^{-9}
2008	17	9.6×10^{-7}	1.0×10^{-8}	9.6×10^{-7}	2.4×10^{-6}	3.6×10^{-9}
2008	20	1.6×10^{-6}	1.1×10^{-8}	1.6×10^{-6}	1.1×10^{-6}	2.6×10^{-9}
2008	21	1.2×10^{-6}	1.9×10^{-8}	1.2×10^{-6}	3.0×10^{-6}	3.6×10^{-9}
2008	22	3.6×10^{-7}	7.0×10^{-9}	3.6×10^{-7}	3.0×10^{-6}	6.0×10^{-9}
2008	25	8.5×10^{-7}	2.4×10^{-8}	8.5×10^{-7}	8.5×10^{-7}	2.1×10^{-9}
2009	1	1.0×10^{-7}	3.7×10^{-9}	9.9×10^{-8}	0.00	0.00
2009	4	6.1×10^{-7}	2.9×10^{-8}	5.8×10^{-7}	2.4×10^{-10}	9.8×10^{-12}
2009	6	1.0×10^{-6}	2.4×10^{-8}	1.0×10^{-6}	3.0×10^{-8}	1.2×10^{-10}
2009	7	5.6×10^{-7}	2.3×10^{-8}	5.4×10^{-7}	3.0×10^{-6}	3.8×10^{-9}
2009	9	1.2×10^{-6}	2.5×10^{-8}	1.2×10^{-6}	3.0×10^{-6}	2.6×10^{-9}
2009	10	6.7×10^{-7}	1.9×10^{-8}	6.5×10^{-7}	0.00	0.00
2009	11	6.7×10^{-7}	3.4×10^{-8}	6.4×10^{-7}	1.7×10^{-6}	2.5×10^{-9}
2009	12[a]	7.6×10^{-7}	1.9×10^{-8}	7.4×10^{-7}	1.5×10^{-7}	5.3×10^{-10}
2009	17	1.8×10^{-6}	7.8×10^{-9}	1.8×10^{-6}	3.7×10^{-7}	5.0×10^{-10}
2009	20	1.3×10^{-6}	5.0×10^{-9}	1.3×10^{-6}	3.8×10^{-8}	1.2×10^{-10}
2009	21	1.8×10^{-6}	9.5×10^{-9}	1.8×10^{-6}	3.6×10^{-7}	5.6×10^{-10}
2009	22	6.7×10^{-7}	1.2×10^{-8}	6.6×10^{-7}	8.8×10^{-7}	1.9×10^{-9}
2009	25[a]	1.2×10^{-6}	3.4×10^{-8}	1.2×10^{-6}	6.3×10^{-8}	1.9×10^{-10}
2010	1	1.1×10^{-7}	2.8×10^{-8}	8.2×10^{-8}	0.00	0.00
2010	4	4.4×10^{-7}	4.0×10^{-7}	4.7×10^{-8}	6.0×10^{-9}	1.6×10^{-10}
2010	6	3.9×10^{-7}	5.0×10^{-8}	3.4×10^{-7}	2.4×10^{-7}	1.4×10^{-9}
2010	7	5.0×10^{-7}	1.2×10^{-7}	3.7×10^{-7}	1.5×10^{-5}	1.0×10^{-8}
2010	9	4.0×10^{-7}	1.9×10^{-7}	2.2×10^{-7}	7.5×10^{-6}	7.6×10^{-9}
2010	10	7.7×10^{-7}	4.2×10^{-7}	3.6×10^{-7}	0.00	0.00
2010	11	6.7×10^{-7}	3.8×10^{-7}	2.9×10^{-7}	1.2×10^{-5}	8.0×10^{-9}
2010	12[a]	3.3×10^{-7}	1.9×10^{-6}	-1.6×10^{-6}	9.9×10^{-7}	3.8×10^{-9}
2010	17	5.5×10^{-7}	2.3×10^{-7}	3.1×10^{-7}	1.6×10^{-6}	3.5×10^{-9}
2010	20	6.8×10^{-7}	4.7×10^{-8}	6.4×10^{-7}	4.2×10^{-7}	1.3×10^{-9}
2010	21	1.0×10^{-6}	1.2×10^{-7}	9.3×10^{-7}	3.1×10^{-6}	3.4×10^{-9}
2010	22	5.0×10^{-7}	5.0×10^{-8}	4.5×10^{-7}	5.6×10^{-6}	1.9×10^{-9}
2010	25[a]	7.4×10^{-7}	2.5×10^{-7}	4.9×10^{-7}	7.4×10^{-7}	1.8×10^{-9}

ANOVA

u_{*_t}	u_{*_t}	Adjusted P value	Different
Uniform	Field	<0.001	Yes
Okin	Field	0.02	No[c]
Okin	Raupach	<0.001	Yes
Field	Raupach	0.005	Yes[c]

[a]Average of two BSNE stems.
[b]Numbers are not normalized or adjusted for homoscedasticity.
[c]Nonparametric ANOVA.

4. Discussion

[37] Many of our plots have experienced periods of groundwater pumping, contributing to the decline of alkali meadow grasses and replacement by shrubs [*Elmore et al*., 2006]. Given previous work that describes the impacts of groundwater pumping on vegetation cover and the cover of perennial grasses in particular [*Elmore et al*., 2003, 2006], we interpret the relationships that we observe between field-measured total horizontal aeolian sediment flux (Q_{field}) of the BSNE stems for 2008 and 2009 and vegetation structure (known to be caused in part by land use change) (Figure 2). The Q_{field} is comparable to other values of Q in similar environments (Minqin, China [*Dong et al*., 2010], and Chihuahaun Desert Playas [*Bergametti and Gillette*, 2010]). Although horizontal transport and dust emission are not always correlated, *Gillette et al*. [1997] showed a relationship between horizontal flux and vertical flux at the Owens Lake, which exhibits similar soils to those found at our plots. This combination of evidence supports the idea that dust emission is occurring at our plots. Plots with intact, continuous grass cover, or taller shrubs with small inter-shrub spaces each exhibited small scaled gap sizes and generally reported the lowest Q (Figure 2d). Groundwater depth is known to influence both the cover of alkali meadow grasses [*Elmore et al*., 2006] and the formation of puffy ground, through evaporation of solute-rich soil moisture [*Gillette et al*., 2001; *Elmore et al*., 2006]. Most research has focused on Owens Lake as the source of dust emission to the valley [*Goudie and Middleton*, 1992; *Cahill et al*., 1996; *Gill*, 1996; *Reheis*, 1997, 2006]; however, as indicated by Figure 2, the wind erosion from the vegetated portion of the valley floor can be considerable.

[38] The λ parameter has been used in wind erosion research since *Marshall* [1971] and has been included in shear stress partitioning models and models of wind erosion

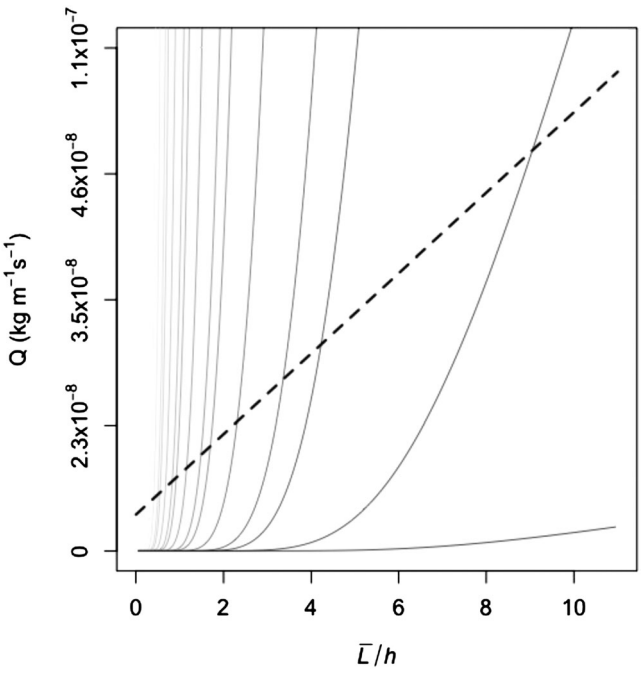

Figure 4. Q increases exponentially with increasing $\bar{L}/h$ across a range of u_{*_t} (light gray (0.2 m s^{-1}) to black (0.6 m s^{-1})). However, $\bar{L}/h$ and Q increase linearly for our plots as in Figure 2d (dashed line). One explanation is that u_{*_t} increases with increasing $\bar{L}/h$, perhaps through wind erosion and surface armoring.

with roughness elements [*Raupach et al*., 1993; *Marticorena and Bergametti*, 1995; *Musick et al*., 1996; *Wolfe and Nickling*, 1996; *Marticorena et al*., 1997; *Dong et al*., 2001]. However, λ parameter was not correlated with Q at our plots (Table 4). We attribute this to the inability of λ to quantify differences between plots with many small roughness elements from plots with few large roughness elements (e.g., compare plots 1 and 10). Several of the other vegetation parameters were likewise not correlated with Q (Table 4) because like the λ parameter, they explained the quantity but not the distribution of roughness elements on the landscape. Scaled gap size, $\bar{L}/h$, on the other hand, was correlated with Q_{field} (Table 4 and Figure 2). The success of $\bar{L}/h$ as a vegetation parameter is due to its ability to describe the heterogeneous distribution of vegetation (e.g., mixture of shrubs, grass, and bare soil gaps) and the amount of sheltered bare soil (i.e., reduced shear wake zone) behind the vegetation [*Okin*, 2008]. The relationship between $\bar{L}/h$ and Q in empirical and process-based models is important in understanding wind erosion in groundwater-dependent meadows.

[39] The most explanatory empirical model predicting Q (equation (11)) utilized two vegetation parameters to model Q ($\bar{L}/h$ and $\bar{L}$) in 2008 and 2009 (but not 2010). Although, $\bar{L}$ was slightly correlated with Q, combining $\bar{L}$ and $\bar{L}/h$ in the regression explained a slightly greater variability in Q, which led to a slight increase in prediction of the model (parameter: $\bar{L}/h$; $R^2 = 0.56$ and parameters: $\bar{L}/h$ and $\bar{L}$; $R^2 = 0.58$). This might occur because together $\bar{L}$ and $\bar{L}/h$ help draw out the differences between grass-dominated and shrub-dominated plots. Extending measurements of $\bar{L}/h$ and the relationship in Figure 2 and equation (11) to estimate Q of other sites in the Owens Valley or elsewhere should be done with extreme caution as variations in soil and vegetation characteristics are more likely to influence this relationship. Where appropriate, Q derived from the described empirical relationships could be used to help managers target areas susceptible to wind erosion. This approach would be valid under the assumption that u_{*_t} and wind fields are the same for all plots.

[40] The Raupach model estimated lower Q values than measured in the field due to the inability of lateral cover to appropriately characterize the vegetation structure at our plots. To obtain Q values from the Raupach model that match Q values obtained from the field, the u_{*_t} of bare soil would have to be lower than both values found in the literature (Table 3) as well as those estimated in the field. However, field measures of u_{*_t} show values similar to literature cited values at comparable plots (Tables 2 and 3). The Okin model does a better job at predicting Q in vegetated landscapes because it represents the distribution of vegetation cover, recognizing that large soil gaps can produce Q despite significant vegetation cover. The mean Q_{Okin} and mean Q_{field} were not significantly different (P of 0.02; Table 5). However, the mean Q_{Unifrom} and Q_{field} were significantly different (Table 5), indicating that a single value of u_{*_t} estimated from literature across this study site is insufficient to characterize the inherent spatial variability. Further, where individual plots reported different Q_{Okin} and Q_{field}, we generally observed a diversity of soil surfaces (salt crusts, packed clay, etc.) and gap sizes (e.g., a few large gaps), suggesting that a single u_{*_t} value for the entire plot might not be appropriate.

[41] The Okin model predicts that as $\bar{L}/h$ increases, the Q response resembles a sigmoid growth pattern. Over the range in $\bar{L}/h$ observed at our plots, a linear relationship between $\bar{L}/h$ and Q can only be achieved if the u_{*_t} increases with increasing $\bar{L}/h$ (Figure 4). In other words, our data support the idea that in this study area, as gaps increase in size, they become increasingly resistant to wind erosion and form streets [*Okin et al*., 2001]. As vegetation cover is diminished in and around gaps, the longer wind fetch enables the erosion of an increasing area leading to increased dust emissions. However, as gaps increase in size, the edges of the gaps maintain loose, easily erodible soil. These observations support our understanding of groundwater influences on Q [*Elmore et al*., 2008]; plots with larger gaps usually have deeper groundwater [*Elmore et al*., 2006], and groundwater depth has been found to be inversely related to dust emissions, at least for playas [*Reynolds et al*., 2007]. Although u_{*_t} is higher in streets, these areas have the ability to produce large amounts of horizontal flux due to a large fetch [*Okin et al*., 2001], causing saltation and dust emission along the length of the street and burying and damaging vegetation on the periphery of the street [*Okin et al*., 2009], leading to increased bare soil area. This study has shown the utility of the Okin model and the measurement of $\bar{L}/h$ to be important in modeling aeolian transport in complex vegetation.

[42] The results from this study are applicable to any environment with sparse vegetation and high wind velocities, but vegetated coastal dunes might be one of the more interesting comparisons. Unvegetated surfaces are seldom found in coastal aeolian environments, but vegetation cover can be spatially variable and dependent on disturbance history [*Alcantara-Carrio and Alonso*, 2002]. Therefore, coastal dune stabilization depends on vegetation cover change [*Levin et al*., 2006], and the degree to which vegetation moderates wind erosion [*Fulbright et al*., 2006]. Wind erosion models that include vegetation parameters such as percent cover and mean vegetation height to characterize vegetation have been effective in modeling these processes [*Buckley*, 1987; *Alcantara-Carrio and Alonso*, 2002; *Levin et al*., 2006], suggesting $\bar{L}/h$ and the Okin model might provide beneficial information in vegetated coastal dune environments.

[43] There are many interesting uncertainties remaining to be investigated, including quantifying the impacts of grazing and other disturbances and understanding the source and consequences of spatial and temporal variability in model parameters influencing Q. Grazing is known to increase the bare soil area and decrease grass height [*Nash et al*., 2004]. Grazing animals also disturb soil crusts enabling wind erosion, particularly along frequently used paths [*Belnap*, 1995]. We saw little evidence that inter-plot variation in grazing intensity influenced vegetation structural differences between our plots and therefore did not attempt to quantify the effect of cattle. This being said, the interpretation of our results does not depend on an understanding of the causes of vegetation structural differences between plots, only on their magnitude and on the relationship between vegetation structure and estimates of Q. Therefore, the most difficult disturbance to incorporate are those that increase the transport of sediment to our plots from locations outside the range of our transects, which extended 50 m from each BSNE stem. For example, it cannot be ruled out that activity on local roads (many of which are unpaved) or off-road all terrain vehicle (ATV) activities had an impact on our measurements and model success [e.g., *Belnap*, 1995]. In Owens Valley, ATVs are permitted on dirt roads located within 500 m of our plots, and roadwork (grading, paving, etc.) is ongoing in many areas. Although it would be hard to measure the impact of these dust sources on measurements of Q at our plots, it is possible they lead to temporal or spatial variability in the success of empirical and mechanistic models to predict Q.

[44] Further refinements to the models used here will likely require a more detailed representation of spatial and temporal variability in model parameters (e.g., u_{*_t}, in particular) and Q. Although we found that measurements of Q were not sensitive to the placement of BSNE stems in 2008 and 2009, the placement in 2010 might have contributed to the increase in Q observed at some plots. This possibility brings into question several assumptions we made regarding the spatial and temporal variability in model parameters. For example, a single value of u_{*_t} was used at each plot, yet we commonly observed loose soil at the edges of gaps in the vicinity of vegetation indicating a range in values exists. Likewise, vegetation structure was measured only at BSNE stem deployment, which does not account for vegetation structural changes throughout the growing season. Finally, we only measured u_{*_t} and Q in the summer, potentially missing significant changes in soil condition and Q during winter (31% of Q events as measured from MET stations). During BSNE stem deployment, wind velocity at 0.5 m exceeded u_{*_t} an average of 60% of the time in 2009 at the two southern MET stations. During 2010, wind velocity exceeded u_{*_t} at our plots an average of 75% of the time at the two southern MET stations, which might explain the greater Q observed in 2010 at some plots. However, this comparison of wind velocity at 0.5 m and u_{*_t} does not take into account the sheltering effect of vegetation. In combination, these unmeasured factors call for work that incorporates spatial and temporal variability in model parameters into models of Q. The strongest empirical model found here explained 58% of the variation in Q, leaving considerable variability for measurements and approaches for estimating Q.

5. Conclusions

[45] Determining which vegetation parameter best relates to Q is important, both for understanding the mechanics of wind erosion models and for using these models to manage for soil stability. In this study, scaled gap size better explained Q than other vegetation parameters including lateral cover, the vegetation parameter most widely used in wind erosion modeling (Table 4). Adding an additional vegetation parameter, gap size, slightly increased the prediction of Q (from 56% to 58% variance explained; equation (11)). These two vegetation parameters are easily measured in the field, therefore offering land and resource managers a useful option when assessing the potential wind erosion at any site. The scaled gap size in particular appears to be a useful metric in systems impacted by disturbance processes that decrease inter-shrub grass cover.

[46] Wind erosion models that use scaled gap size instead of lateral cover are more successful in predicting Q in areas of heterogeneous vegetation. The Okin model, using scaled gap size, better predicted Q_{field} than the commonly used Raupach model, using λ (Table 5), suggesting the Okin model should be used where vegetation cover is spatially heterogeneous. However, predictive capability of the Okin model using a single average u_{*_t} for all plots ($0.56\,\text{m}\,\text{s}^{-1}$; Table 3) overestimated Q (Table 5), demonstrating the importance of knowing u_{*_t} at each plot. Further, across our study plots, u_{*_t} correlated with bare soil area, which is consistent with the idea that soil surfaces in large gaps become more resistant to erosion over time. Practical applications of the Okin model might use a range of u_{*_t} values to produce a range of potential Q values, or attempt to parameterize u_{*_t} as a function of bare soil area. Further, modeling work might benefit by taking into account within-plot variability in u_{*_t}. For example, u_{*_t} could be varied based upon gap size and position within a gap.

[47] Natural resource managers can use both the Okin model and simple empirical models to target management actions in alkali meadow vegetation. Wind erosion causes reduced soil fertility that is unfavorable to vegetation reestablishment [*Belnap and Gillette*, 1998; *Li et al*., 2007; *Elmore et al*., 2008] eventually forming streets and areas of reduced fertility [*Okin et al*., 2001; *McGlynn and Okin*, 2006]. Continued disturbance of vegetation in Owens valley, for example, has the potential to cause the formation of streets, elevating u_{*_t} as bare soils become more common and allowing for a longer fetch for saltation and dust emission, thus burying and damaging plants and creating more

bare soil area [*Okin et al*., 2001, 2009]. Understanding the interaction of soil resources, groundwater depth, and vegetation structure may illuminate whether wind erosion promotes these positive feedbacks eventually leading to desertification, increased dust emissions, reduced air quality, and associated human health problems.

[48] **Acknowledgments.** This work was funded by the National Science Foundation (Award #EAR0719793) and by a graduate mini-grant from the White Mountain Research Station, University of California.

References

Alcantara-Carrio, J., and I. Alonso (2002), Measurement and prediction of aeolain sediment transport at Jandia Isthmus (Fuerteventura, Canary Islands), *J. Coastal Res*, *18*(2), 300–315.

Aubault, H. (2009), Impacts modeling of change textures due to groundwater decline on the dust emission rates, Owens Valley (California), Université Paris 7 - Diderot, Paris, France.

Belnap, J. (1995), Surface disturbances: Their role in accelerating desertification, *Environ. Monit. Assess.*, *37*, 39–57, doi:10.1007/BF00546879.

Belnap, J., and D. Gillette (1998), Vulnerability of desert biological soil crusts to wind erosion: The influences of crust development, soil texture, and disturbance, *J. Arid Environ.*, *39*(2), 133–142, doi:10.1006/jare.1998.0388.

Bergametti, G., and D. A. Gillette (2010), Aeolian sediment fluxes measured over various plant/soil complexes in the Chihuahuan desert, *J. Geophys. Res.*, *115*, F03044, doi:10.1029/2009JF001543.

Breshears, D. D., J. J. Whicker, C. B. Zou, J. P. Field, and C. D. Allen (2009), A conceptual framework for dryland aeolian sediment transport along the grassland-forest continuum: Effects of woody plant canopy cover and disturbance, *Geomorphol.*, *105*(1-2), 28–38, doi:10.1016/j.geomorph.2007.12.018.

Brown, S., W. G. Nickling, and J. A. Gillies (2008), A wind tunnel examination of shear stress partitioning for an assortment of surface roughness distributions, *J. Geophys. Res.*, *113*, F02S06, doi:10.1029/2007JF000790.

Buckley, R. (1987), The effect of sparse vegetation on the transport of dune sand by wind, *Nature*, *325*, 426–428.

Cahill, T. A., T. E. Gill, J. S. Reid, E. A. Gearhart, and D. A. Gillette (1996), Saltating particles, playa crusts and dust aerosols at Owens (dry) Lake, California, *Earth Surf. Processes Landforms*, *21*(7), 621–639.

Danskin, W. R. (1998), Evaluation of the hydrologic system and selected water-management alternatives in the Owens Valley, California, United States Geological Survey, Washington, DC.

Dong, Z. B., S. Y. Gao, and D. W. Fryrear (2001), Drag coefficients, roughness length and zero-plane displacement height as disturbed by artificial standing vegetation, *J. Arid Environ.*, *49*(3), 485–505, doi:10.1006/jarc.2001.0807.

Dong, Z., D. Man, W. Luo, G. Qian, J. Wang, M. Zhao, S. Liu, G. Zhu, and S. Zhu (2010), Horizontal aeolian sediment flux in the Minqin area, a major source of Chinese dust storms, *Geomorphol.*, *116*, 58–66, doi:10.1016/j.geomorph.2009.10.008.

Elmore, A. J., J. F. Mustard, S. J. Manning, and D. B. Lobell (2000), Quantifying vegetation change in semiarid environments: Precision and accuracy of spectral mixture analysis and the normalized difference vegetation index, *Remote Sens. Environ.*, *73*(1), 87–102, doi:10.1016/S0034-4257(00)00100-0.

Elmore, A. J., J. F. Mustard, and S. J. Manning (2003), Regional patterns of plant community response to changes in water: Owens Valley, California, *Ecol. Appl.*, *13*, 443–460, doi:10.1890/1051-0761(2003)013[0443:RPOPCR]2.0.CO;2.

Elmore, A. J., S. J. Manning, J. F. Mustard, and J. M. Craine (2006), Decline in alkali meadow vegetation cover in California: The effects of groundwater extraction and drought, *J. Appl. Ecol.*, *43*(4), 770–779, doi:10.1111/j.1365-2664.2006.01197.x.

Elmore, A. J., J. M. Kaste, G. S. Okin, and M. S. Fantle (2008), Groundwater influences on atmospheric dust generation in deserts, *J. Arid Environ.*, *72*, 1753–1765, doi:10.1016/j.jaridenv.2008.05.008.

Fryrear, D. W. (1985), Soil cover and wind erosion, *Trans. ASEA*, *28*(3), 781–784.

Fulbright, T. E., J. A. Ortega-Santos, A. Lozano-Cavazos, and L. E. Ramirez-Yanez (2006), Establishing vegetation on migrating inland sand dunes in Texas, *Rangel. Ecol. Manage.*, *59*(5), 549–556.

Gill, T. E. (1996), Eolian sediments generated by anthropogenic disturbance of playas: Human impacts on the geomorphic system and geomorphic impacts on the human system, *Geomorphol.*, *17*(1-3), 207–228, doi:10.1016/0169-555(95)00104-D.

Gillette, D. A. (1997), Soil derived dust as a source of silica: Aerosol properties, emissions, deposition, and transport, *J. Expo. Anal. Environ. Epidemiol.*, *7*(3), 303–311.

Gillette, D. A., and R. Passi (1988), Modeling dust emission caused by wind erosion, *J. Geophys. Res.*, *93*(D11), 14233–14242, doi:10.1029/JD093iD11p14233.

Gillette, D. A., J. Adams, A. Endo, D. Smith, and R. Kihl (1980), Threshold velocities for input of soil particles into the air by desert soils, *J. Geophys. Res.*, *85*(NC10), 5621–5630, doi:10.1029/JC085iC10p05621.

Gillette, D. A., J. Adams, D. Muhs, and R. Kihl (1982), Threshold friction velocities and rupture moduli for crusted desert soils for the input of soil particles into the air, *J. Geophys. Res.*, *87*(C11), 9003–9015, doi:10.1029/JC087iC11p09003.

Gillette, D. A., D. W. Fryrear, T. E. Gill, T. Ley, T. A. Cahill, and E. A. Gearhart (1997), Relation of vertical flux of particles smaller than 10 μm to total aeolian horizontal mass flux at Owens Lake, *J. Geophys. Res.*, *102*(D22), 26009–26015, doi:10.1029/97JD02252.

Gillette, D. A., T. C. Niemeyer, and P. J. Helm (2001), Supply-limited horizontal sand drift at an ephemerally crusted, unvegetated saline playa, *J. Geophys. Res.*, *106*(D16), 18085–18098, doi:10.1029/2000JD900324.

Gillette, D. A., J. E. Herrick, and G. A. Herbert (2006), Wind characteristics of mesquite streets in the northern Chihuahuan Desert, New Mexico, USA, *Environ. Fluid Mech.*, *6*(3), 241–275.

Goudie, A. S., and N. J. Middleton (1992), The changing frequency of dust storms through time, *Clim. Chang.*, *20*(3), 197–225, doi:10.1007/BF00139839.

Hollett, K. J., W. R. Danskin, W. F. McCaffrey, and C. L. Walti (1991), Geology and water resources of Owens Valley, California, United States Geological Survey, Washington, DC.

James, G., D. Groeneveld, B. Hutchinson, D. C. Williams, R. H. Rawson, and E. L. Coufal (1990), Technical appendix F green book for the long-term groundwater management plan for the Owens Valley and Inyo County, in Draft EIR: Water from the Owens Valley to Supply the Second Los Angeles Aqueduct; 1970 to 1990, and 1990 Onward, Pursuant to a Long Term Groundwater Management Plan, Department of Water and Power, City of Los Angeles, Calif.

King, J., W. G. Nickling, and J. A. Gillies (2005), Representation of vegetation and other nonerodible elements in aeolian shear stress partitioning models for predicting transport threshold, *J. Geophys. Res.*, *110*, F04015, doi:10.1029/2004JF000281.

Lancaster, N., and A. Baas (1998), Influence of vegetation cover on sand transport by wind: Field studies at Owens Lake, California, *Earth Surf. Processes Landforms*, *23*(1), 69–82.

Levin, N., G. J. Kidron, and E. Ben-Dor (2006), The spatial and temporal variability of sand erosion across a stabilizing coastal dune field, *Sedimentology*, *53*, 697–715, doi:10.1111/j.1365-3091.2006.00787.x.

Li, J., G. S. Okin, L. Alvarez, and H. Epstein (2007), Quantitative effects of vegetation cover on wind erosion and soil nutrient loss in a desert grassland of southern New Mexico, USA, *Biogeochem.*, *85*, 317–332, doi:10.1007/s10533-007-9142-y.

Li, J., G. S. Okin, J. E. Herrick, J. Belnap, S. M. Munson, and M. E. Miller (2010), A simple method to estimate threshold friction velocity of wind erosion in the field, *Geophys. Res. Lett.*, *37*, L10402, doi:10.1029/2010GL043245.

Li, L., L. Shaomin, X. Zeiwei, Y. Kun, C. Xuhui, J. Li, and J. Wang (2009), The characteristics and parameterization of aerodynamic roughness length over heterogeneous surfaces, *Adv. Atmos. Sci.*, *26*(1), 180–190, doi:10.1007/s00376-009-0180-3.

Marshall, J. K. (1971), Drag measurements in roughness arrays of varying density and distribution, *Agric. Meteorol.*, *8*(4-5), 269–292, doi:10.1016/0002-1571(71)90116-6.

Marticorena, B., and G. Bergametti (1995), Modeling the atmospheric dust cycle: 1. Design of a soil-derived dust emission scheme, *J. Geophys. Res.*, *100*(D8), 16415–16430, doi:10.1029/95JD00690.

Marticorena, B., G. Bergametti, B. Aumont, Y. Callot, C. NDoume, and M. Legrand (1997), Modeling the atmospheric dust cycle. 2. Simulation of Saharan dust sources, *J. Geophys. Res.*, *102*(D4), 4387–4404, doi:10.1029/96JD02964.

Mata-Gonzalez, R., T. McLendon, D. W. Martin, M. J. Trica, and R. A. Pearce (2012). Vegetation as affected by groundwater depth and microtopography in a shallow aquifer area of the Great Basin, *Ecohydrol.*, *5*(1), 54–63, doi:10.1002/eco.196.

McGlynn, I. O., and G. S. Okin (2006), Characterization of shrub distribution using high spatial resolution remote sensing: Ecosystem implications for a former Chihuahuan Desert grassland, *Remote Sens. Environ.*, *10*(4), 554–566.

Musick, H. B., and D. A. Gillette (1990), Field evaluation of relationships between a vegetation structural parameter and sheltering against wind erosion, *Land Degrad.and Rehabil.*, *2*(2), 87–94.

Musick, H. B., S. M. Trujillo, and C. R. Truman (1996), Wind-tunnel modelling of the influence of vegetation structure on saltation threshold, *Earthquake Eng. Struct. Dyn*, *21*(7), 589–605.

Nash, M. S., E. Jackson, and W. G. Whitford (2004), Effects of intense, short-duration grazing on microtopography in a Chihuahan Desert grassland, *J. Arid Environ.*, *56*(3), 383–393, doi:10.1016/S0140-1963(03)00062-4.

Nickling, W. G., and C. M. Neuman (1997), Wind tunnel evaluation of a wedge-shaped aeolian sediment trap, *Geomorphol.*, *18*, 333–345.

Okin, G. S. (2005), Dependence of wind erosion and dust emission on surface heterogeneity: Stochastic modeling, *J. Geophys. Res.*, *110*(D11), doi:10.1029/2004JD005288.

Okin, G. S. (2008), A new model of wind erosion in the presence of vegetation, *J. Geophys. Res.-Earth Surf.*, *113*(F2), doi:10.1029/2007JF000758.

Okin, G. S., and D. A. Gillette (2001), Distribution of vegetation in wind-dominated landscapes: Implications for wind erosion modeling and landscape processes, *J. Geophys. Res.*, *106*(D9), 9673–9683, doi:10.1029/2001JD900052.

Okin, G. S., B. Murry, and W. H. Schlesinger (2001), Degradation of sandy arid shrubland environments: Observations, process modelling, and management implications, *J. Arid Environ.*, *47*(2), 123–144, doi:10.1006/jare.2000.0711.

Okin, G. S., D. A. Gillette, and J. E. Herrick (2006), Multi-scale controls on and consequences of aeolian processes in landscape change in arid and semi-arid environments, *J. Arid Environ.*, *65*(2), 253–275, doi:10.1016/j.jaridenv.2005.06.029.

Okin, G. S., A. J. Parsons, J. Wainwright, J. E. Herrick, B. T. Bestelmeyer, D. C. Peters, and E. L. Fredrickson (2009), Do changes in connectivity explain desertification?, *Bioscience*, *59*(3), 237–244, doi:10.1525/bio.2009.59.3.8.

Orme, A. R., and A. J. Orme (2008), Late Cenozoic drainage history of the southwestern Great Basin and lower Colorado River region: Geologic and biotic perspectives, Geological Society of America, Boulder, Colorado.

Park, S., and H. In (2003), Parameterization of dust emission for the simulation of the yellow sand (Asian dust) event observed in Marsh 2002 in Korea, *J. Geophys. Res.*, *108*(D19), 4618, doi:10.1029/2003JD003484.

Peters, D. P., B. T. Bestelmeyer, J. E. Herrick, E. L. Fredrickson, H. C. Monger, and K. M. Havstad (2006), Disentangling complex landscapes: New insights into arid and semiarid system dynamics, *Bioscience*, *56*(6), 491–501, doi:10.1641/0006-3568(2006)56[491:DCLNII]2.0.CO;2.

Priestley, C. H. B. (1959), Estimation of surface stress and heat flux from profile data, *Q. J. R. Meteorolog. Soc.*, *85*(366), 415–418, doi:10.1002/qj.49708536611.

Prigent, C., I. Tegen, F. Aires, B. Morticorena, and M. Zribi (2005), Estimation of the aerodynamic roughness length in arid and semi-arid regions over the globe with the ERS scatterometer, *J. Geophys. Res.*, *110*, D09205, doi:10.1029/2004JD005370.

Raab, T., and G. Mayr (2008), Hydraulic interpretation of the footprints of Sierra Nevada windstorms tracked with an automobile measurement system, *J. Appl. Meteorol. Climatol.*, *47*, 2581–2599, doi:10.1175/2008JAMC1675.1.

Raupach, M. R. (1992), Drag and drag partition on rough surfaces, *Boundary Layer Meteorol.*, *60*(4), 375-395, doi:10.1007/BF00155203.

Raupach, M. R., D. A. Gillette, and J. F. Leys (1993), The effect of roughness elements on wind erosion threshold, *J. Geophys. Res.*, *98* (D2), 3023–3029, doi:10.1029/92JD01922.

Reheis, M. C. (1997), Dust deposition downwind of Owens (dry) Lake, 1991–1994: Preliminary findings, *J. Geophys. Res.*, *102*(D22), 25999–26008, doi:10.1029/97JD01967.

Reheis, M. C. (2006), A 16-year record of eolian dust in Southern Nevada and California, USA: Controls on dust generation and accumulation, *J. Arid Environ.*, *67*(3), 487–520, doi:10.1016/j.jaridenv.2006.03.006.

Reheis, M. C., J. R. Budahn, P. J. Lamothe, and R. L. Reynolds (2009), Compositions of modern dust and surface sediments in the Desert Southwest, United States, *J. Geophys. Res.*, *114*, F01028, doi:10.1029/2008JF001009.

Reynolds, R. L., J. C. Yount, M. C. Reheis, H. Goldstein, J. Chavez, R. Fulton, J. Whitney, C. Fuller, and R. M. Forester (2007), Dust emission from wet and dry playas in the Mojave desert, USA, *Earth Surf. Processes Landforms*, *32*(12), 1811–1827, doi:10.1002/esp.1515.

Rodriquez-Caballero, E., Y. Canton, S. Chamizo, A. Afana, and A. Sole-Benet (2012), Effects of biological soil crusts on surface roughness and implications for runoff and erosion, *Geomorphol.*, *145-146*, 81–89, doi:10.1016/j.geomorph.2011.12.042.

Saint-Amand, P., C. Gaines, and D. Saint-Amand (1987), Owens Lake, an ionic soap opera staged on a natric playa, Special Field Guide—Cordileran Section, Geological Society of America, Boulder, Colorado.

Schlesinger, W. H., J. F. Reynolds, G. L. Cunningham, L. F. Huenneke, W. M. Jarrell, R. A. Virginia, and W. G. Whitford (1990), Biological feedbacks in global desertification, *Science*, *247*(4946), 1043–1048.

Shao, Y. P. (2000), Physics and Modeling of Wind Erosion, Kluwer Academic Publishers, Norwell, Massachusetts.

Shao Y. P., and M. R. Raupach (1992), The overshoot and equilibration of saltation, *J. Geophys. Res.*, *97*(D18), 20559–20564, doi:10.1029/92JD02011.

Shao, Y. P., G. H. McTainsh, J. F. Leys, and M. R. Raupach (1993), Efficiencies of sediment samplers for wind erosion measurement, *Aust. J. Soil Res.*, *31*(4), 519–532, doi:10.1071/SR9930519.

Shao, Y., M. Ishizuka, M. Mikami, and J. F. Leys (2011), Parameterization of size-resolved dust emission and validation with measurements, *J. Geophys. Res.*, *116*(D8), doi:10.1029/2010JD014527.

Soil Survey Staff (2006), Natural Resources Conservation Service, United States Department of Agriculture, *Soil Survey Geographic* (*SSURGO*) *Database for* [*CA732*, *California]*. [online] Available from: http://soildatamart.nrcs.usda.gov accessed [4/15/2010]

Sorenson, S., P. Dileanis, and F. Branson (1991), Soil and vegetation response to precipitation and changes in depth to groundwater in Owens Valley., US Geological Survey, Washington, DC.

USDA, and NRCS (2004), Chapter 16—Line point transects for basal and canopy gaps, National Resources Inventory Handbook of Instructions for Rangeland Field Study Data Collection, U.S. Department of Agriculture, Washington DC.

Wolfe, S. A., and W. G. Nickling (1996), Shear stress partitioning in sparsely vegetated desert canopies, *Earth Surf. Processes Landforms*, *21* (7), 607–619.